Wavelength references for interferometry in air

Richard W. Fox, Brian R. Washburn, Nathan R. Newbury, and Leo Hollberg

Cavity-mode wavelengths in air are determined by measuring a laser's frequency while it is locked to the mode in vacuum during a calibration step and subsequently correcting the mode wavelength for atmospheric pressure compression, temperature difference, and material aging. Using a Zerodur ring cavity, we demonstrate a repeatability of $\pm 2 \times 10^{-8}$ (3σ), with the wavelength accuracy limited to $\pm 4 \times 10^{-8}$ by knowledge of the absolute helium gas temperature during the pressure calibration. Mirror cleaning perturbed the mode frequency by less than $\Delta\nu/\nu \sim 3 \times 10^{-9}$, limited by temperature correction residuals. © 2005 Optical Society of America

OCIS codes: 120.2230, 120.3180, 120.3940.

1. Introduction

Commercial frequency-stabilized He–Ne lasers typically have a frequency uncertainty of a few parts in 10^8 or smaller, and in vacuum the laser beam's wavelength uncertainty ($\Delta\lambda/\lambda$) is fractionally equivalent, although of opposite sign. The wavelength uncertainty $\Delta\lambda/\lambda$ is appreciably larger in air owing to uncertainties in the index of refraction, which can affect the accuracy and repeatability of interferometric measurements. There are of course many other potential errors of interferometric measurement, such as cosine error, Abbé error, dead-path error, polarization-mixing nonlinearities, and thermal drifts of the optics. However, especially for longer interferometer path lengths, wavelength uncertainty can be a significant part of the error budget.

Air movement causes fluctuations of the refractive index and hence of wavelength that increase the variance of the interferometer's phase in a given measurement interval or averaging time. The measurement precision is often limited by these wavelength fluctuations in applications with air flow and relatively short averaging times, for instance, motion stages.[1] Consequently, increasingly precise knowledge of the average wavelength over a longer time interval is generally not useful unless the fluctuations can be reduced or compensated for in some way. Low-finesse air-spaced etalons of arbitrary length are sometimes used for compensation,[2] but absolute accuracy requires information from another source, such as measuring a known standard with the interferometer system or estimating the average wavelength from environmental measurements. Two-color techniques that derive changes in the refractivity from interferometric measurements of the same path at different colors have also been shown to reduce fluctuations.[1] The degree of compensation will depend on the correlation between the air in the actual measurement path and the compensation path.[3]

Most often the beam's average wavelength is determined by use of a refractive-index model and careful measurements of the air's environmental parameters. Agreement of a model with refractivity measurements has been shown to at least a few parts in 10^8.[4] However, to achieve a wavelength uncertainty (3σ) of even 1 part in 10^7 by this method in a routine manner in an industrial setting is not trivial. For instance, this task requires *absolute* measurement of the average air temperature along the interferometer path to ± 100 m°C. Such accuracy requires careful calibration at regular intervals and attention to error sources such as self-heating of the thermistor or platinum resistance temperature detector, which is air-flow velocity dependent.

An alternative approach of using one or more resonances of a stable optical cavity to provide wavelength information in air has been explored in recent years.[5–9] In a manner similar to etalon-based compensation, a moderate finesse cavity can offer reduced wavelength fluctuations but can also supply accurately known wavelengths without the need for precision air-temperature measurements (Fig. 1). The wavelength and frequency of a cavity mode are

The authors are with the National Institute of Standards and Technology, 325 Broadway, Boulder, Colorado 80305. R. W. Fox's e-mail address is richard.fox@nist.gov.

Received 6 April 2005; accepted 31 May 2005.
0003-6935/05/367793-09$15.00/0

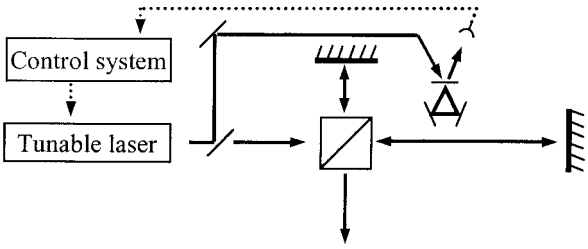

Fig. 1. Example of a cavity wavelength reference used with a homodyne Michelson interferometer. A portion of the interferometer source illuminates a triangular three-mirror air-spaced reference cavity, and the tunable laser is electronically servocontrolled to remain locked to a cavity mode that has a known wavelength. The reference cavity is placed in close vicinity to the interferometer beams to maximize the correlation between the refractive index of the air in the cavity and in the interferometer path.

approximately $\lambda = L/m$ and $\nu = mc/nL$, respectively (m represents the mode number, L the round-trip path length, and n the index of refraction). With a tunable laser locked to a cavity mode, the wavelength of the light in the cavity remains constant because the laser's frequency is adjusted (inversely) proportionally to any index-of-refraction change of the air in the cavity. In particular, length measurements have been demonstrated by use of a Fabry–Perot cavity wavelength reference at 633 nm that was calibrated with an iodine-stabilized He–Ne laser.[7] The technologies to create stable reference cavities, tunable lasers, and locking electronics have been available for some time, although the means to measure easily the frequencies of arbitrary reference modes and therefore the mode wavelengths has not.

Now, with the advent of femtosecond comb frequency measurements,[10] a cavity mode's resonant frequency and hence wavelength can easily be measured in vacuum during a calibration step. Subsequently, in air, the cavity mode can serve as a wavelength reference as long as any vacuum-to-air change of the physical size is properly accounted for. In fact, a number of small corrections are necessary to compensate for changes in size since calibration. The corrections and their maximum magnitudes are for atmospheric pressure compression ($\Delta L/L = \Delta\lambda/\lambda \approx 10^{-6}$), temperature ($\approx 10^{-7}$), and material aging ($\approx 10^{-7}$). These value's are quite small compared to the air's refractivity ($\approx 2 \times 10^{-4}$) that must be compensated for when one is using a frequency-stabilized laser to provide a known wavelength in air. In addition, this method can provide several accurately known wavelengths simultaneously, facilitating multiple-wavelength interferometry applications. The primary challenges to obtaining air-wavelength uncertainties approaching $\Delta\lambda/\lambda \sim 10^{-8}$ appear to be an accurate accounting of the cavity's contraction caused by atmospheric pressure[11] and, as we discuss here, the ability to measure properly the effective temperature of the low-thermal-conductivity cavity spacer. Periodic calibrations, similar to those required for other precision instruments, may be necessary to ensure the highest accuracy.

In this paper we demonstrate the absolute calibration of a mode wavelength by means of femtosecond-comb frequency measurements and present frequency measurements spanning eight months. We also present cavity-mode frequency measurements before and after the mirrors are cleaned, as contamination of the mirror surfaces appears to be an important issue in the design of absolute resonant air-wavelength references. The paper is organized as follows: First, in Section 2 we discuss resonant wavelength references. In Section 3 we present our method of optical frequency measurement the apparatus used; the measurements are reported and discussed in Section 4.

2. Cavity Wavelength References

High-quality wavelength reference cavities would be fabricated from a low-thermal-expansion spacer and optically contacted or silicate-bonded mirrors.[12] We have fabricated cavities by using both Zerodur[13] and ULE glass[14] as the spacer material, but the frequency measurements reported in this paper pertain to the Zerodur cavities only. We consider ring cavities exclusively, as this reduces optical feedback problems and avoids the use of expensive optical isolators. We can write the resonant wavelength of an optical cavity TEM_{00} mode as

$$\lambda_m = L \Big/ \left[m - \frac{\varphi(\lambda) + \psi_G}{2\pi} \right], \tag{1}$$

where λ_m is the wavelength of the light in the cavity, or in air with the same refractive index as the cavity medium. L is the round-trip physical path length, m is the longitudinal mode index, and $\varphi(\lambda)$ is the cumulative phase shift that is due to reflection accumulated during a single round trip of the cavity. ψ_G represents the geometry-dependent Gouy phase shift over a single round trip of the cavity.[15] Equation (1) is the direct result of requiring an integer number of phase cycles in one round trip of the cavity, $(2\pi L)/\lambda + \varphi(\lambda) + \psi_G = 2\pi m$. We discuss the stability of each variable in Eq. (1) to gain insight into how stable λ_m can be. Our present research has utilized modes with $m \geq 1.7 \times 10^5$, a 25 cm ring-cavity path length, and $\lambda \sim 1.48\ \mu m$, chosen because of the availability of low-cost high-power ($\sim$20 mW) fiber-coupled distributed-feedback (DFB) lasers. Returning a tunable laser to the previously calibrated mode (same longitudinal mode index m) is an important consideration, and a simple method to accomplish this by use of a small auxiliary air-spaced cavity has been demonstrated at 633 nm.[7]

The denominator terms $\varphi(\lambda)/2\pi$ and $\psi_G/2\pi$ are of the order of 1 or less; thus a wavelength uncertainty of $\Delta\lambda/\lambda < 10^{-8}$ requires only $\sim$0.1% stability of these terms between calibrations, as is evident by inspection of Eq. (1) with L and m constant (and large). With regard to the stability of the phase shift on reflection, we are utilizing mirrors with ion-beam sputtered dielectric coatings of Ta_2O_5 and SiO_2. Such coatings are dense, nonporous, and environmentally stable and

may easily be cleaned without damage. We have no evidence that significant changes in the reflection phase shift owing to humidity or other environmental factors occur, but we note that tests of the actual wavelength stability in air or tests with cavities of different lengths[8] will be required for proof of the validity of this statement. Any temperature dependence of the coating phase shift is included in the cavity temperature compensation. The Gouy phase shift is slightly wavelength dependent; however, the change is completely negligible here because the reference mode's actual (uncorrected) wavelength is sufficiently stable.

In practical terms, the wavelength stability of the reference depends on how well the temperature, pressure, and aging dependence of cavity length L can be compensated for. The cavity's temperature dependence can be determined by several measurements over a near-room-temperature range, and subsequent temperature monitoring allows a first-order correction to be made in the wavelength. Such passive monitoring seems preferable to active temperature control, which would perturb the surrounding air temperature. With temperature sensors permanently bonded to the wavelength reference before calibration, only the sensor's repeatability, not the absolute accuracy, is important. In fact, although cavity temperature and atmospheric pressure must be monitored and compensated for to account for any changes of the cavity length, the required accuracy of these environmental measurements is far less than is necessary to gain the same performance from a refractive-index model.

Indeed, one can estimate a reference wavelength uncertainty owing to temperature of $\Delta\lambda/\lambda \leq \pm 1 \times 10^{-9}$ by using a nominal temperature coefficient of $\alpha = \pm 20 \times 10^{-9}$ /°C together with an uncertainty of the relative temperature difference since calibration of ±0.05 °C. However, we show results in Section 4 below that suggest that temperature-related issues limit the resolution of our present system to $\Delta\lambda/\lambda \leq \pm 2 \times 10^{-8}$ (3σ). This corresponds (through the measured temperature coefficient) to an effective path-length temperature uncertainty of ±0.5 °C, far above the random noise level of the array of temperature transducers fixed to the cavity. We believe that the temperature compensation is limited by our temperature sensing of only six discrete points of a 25 cm path length in a low-thermal-conductivity structure and also by thermal hysteresis of the Zerodur spacer. Note that to meet even this nonoptimum level of performance by way of index-of-refraction calculations is hardly possible, as it would require an *absolute-temperature* measurement of the air accurate to ±20 m°C along with confidence that the refractive-index model was valid to this precision.

Likewise, practical considerations limit the ability to compensate, or correct, for the wavelength shift that is due to the pressure-induced contraction of the cavity. The theory of mechanical deformation of simple structures under isotropic pressure is well known.[11] The linear contraction under pressure of 10^5 Pa (760 Torr) is approximately $\Delta L/L \sim 10^{-6}$ in the case of ULE glass and almost a factor of 2 smaller for Zerodur. Thus for ULE it would seem that a pressure measurement accurate to 1% would be adequate to correct the reported wavelength (measured in vacuum) to atmospheric pressure with a fidelity of $\Delta\lambda/\lambda \leq 10^{-8}$. However, to calculate the change in the cavity size (and hence in the mode wavelength) to a precision of $\Delta L/L \sim 10^{-8}$ based on theory would require knowledge of Young's modulus and Poisson's ratio accurate to 1% and 2%, respectively. These parameters are not guaranteed so precisely by the glass manufacturers. The change in cavity size can also be determined by frequency-shift measurements in conjunction with refractive-index measurements.

However, we were not certain that we could measure the absolute average index of refraction of air in the cavity path to much better than 1 part in 10^7. Therefore we measured the pressure-induced contraction by placing the cavity in a pure helium environment. Helium is an excellent choice because its refractivity $(n - 1)$ is nearly a factor of 10 lower than that of air ($n_{\mathrm{He}} = 1.0000324$ at 20 °C, 10^5 Pa, 632.8 nm) and from first-principle calculations is known to approximately the 10^{-10} level.[16] As Stone and Stejskal[16] pointed out, the attainable uncertainty of the refractive index would normally be set by the pressure or temperature measurement of the helium gas, or by impurities in the gas. Our present wavelength uncertainty is limited by the absolute-temperature uncertainty (±0.4 °C) of the helium gas used to calibrate the pressure change.

Wavelength correction for changes in physical length of the cavity path length owing to aging of the glass is relatively important with Zerodur, a glass ceramic material. Optical resonator length contraction of the order of $\Delta L/L \sim 10^{-7}$ per year for new Zerodur cavities with optically contacted mirrors has been observed.[17] For ULE cavities held isothermally in vacuum, apparent aging rates of $\leq -3.7 \times 10^{-9}$ year^{-1} (Ref. 18) and $\leq -5.5 \times 10^{-9}$ year^{-1} (Ref. 19) have been observed. Periodic frequency measurements allow us to remove the first-order trend, as we demonstrate in Section 4 with a logarithmic fit to the Zerodur cavity frequency-versus-time data. With regard to a wavelength reference fabricated with ULE, we expect that the uncertainties after correction will be limited by temperature-associated effects rather than aging.

Contamination of the mirror surfaces in air is a potential error source of a cavity-based wavelength reference. The magnitude of the potential problem will scale inversely with cavity size and will be influenced by the operating environment. In a typical room environment, water molecules will be present in large quantities on the mirror surface. Simple analysis of $L \sim 25$ cm length cavities indicates that several molecular layers of water will not be a signif-

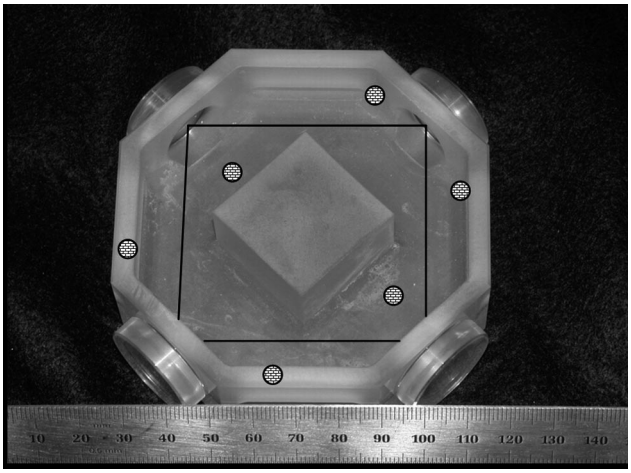

Fig. 2. Beam path and locations of the temperature sensors are superimposed upon this photo of the Zerodur optical cavity wavelength reference. A moderately sized cavity (25.2 cm round-trip path) was chosen to reduce the influence of mirror contamination. Six temperature sensors were bonded with thermally conductive epoxy to monitor the effective temperature of the cavity. The Zerodur base is 7.6 mm thick, and the sidewalls are 5 mm thick. All the inside corners were filleted and, following standard glass-fabrication procedures, the part was acid treated after milling to improve the glass strength. The average temperature (to 1 mK resolution) of the six sensors was recorded during each frequency measurement.

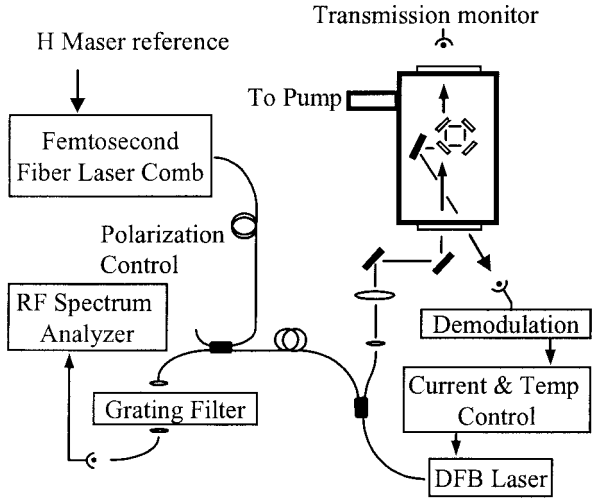

Fig. 3. Experimental diagram showing the cavity in a vacuum chamber with external alignment mirrors. The cavity was placed in the chamber unclamped upon a thin Teflon surface to prevent distortion caused by stress and temperature differences, with repeatable positioning to ease beam alignment provided by a metal stop. A DFB laser was locked to a cavity mode by injection current modulation by the Pound–Drever–Hall technique.[20] A fraction of the light was transmitted via fiber to a femtosecond laser comb some 200 m away for an optical frequency measurement.

icant error term. Even so, we note that our frequency measurements are performed in only a moderate vacuum ($\leq$0.1 Pa) without baking, and significant water is still present on the mirror surfaces during the measurement. Consequently the vacuum wavelength calibration to a large extent should account for the surface water. Perhaps more important is the effect of the ever-present dust and room particulate settling on the mirrors. Advantageous cavity designs will protect the mirrors while at the same time permitting a free flow of air and easy mirror cleaning.

The cavity described here (Fig. 2) is a rectangular ring resonator with a path length of 25.2 cm that has four Zerodur mirrors optically contacted to a Zerodur spacer. (Note: The material was standard Zerodur, not Zerodur-M.) ULE glass is a preferable candidate material in terms of aging, possible temperature-induced hysteresis, and also transmission at 1479 nm; however, Zerodur was used for this prototype cavity because of other nontechnical constraints. We specifically chose a four-mirror, 45° angle of incidence design to study the cavity's polarization-dependent dispersion characteristics in addition to the frequency measurements that we are reporting on here. The mirror mounting surfaces were specified in a square pattern with a tolerance of $\pm$5 arc min that earlier tests showed would be sufficient to achieve cavity alignment by adjustment of the input beam alone. Two of the mirrors are flat, while the other two have a 50 cm curvature, and all the mirrors have the same 99.5% front–side reflectivity (at 1479 nm) with a rear antireflection coating.

3. Frequency Measurement Apparatus

We determined the wavelength of a mode of the reference cavity by measuring the optical frequency of the mode in vacuum. We performed our optical frequency measurements by locking a test laser to the wavelength reference cavity mode and measuring the heterodyne beat note frequency between the test laser and a femtosecond laser comb mode. An experimental diagram is shown in Fig. 3. In this section, first we discuss the relationship of the test laser to the reference cavity-mode center and then we discuss the heterodyne beat identification and measurement.

A. Test-Laser Lock Considerations

We have chosen by design a cavity-mode linewidth of no more than a few parts in 10^8 so that certain locking issues are rendered unimportant for the wavelength reference performance. For instance, one can accomplish locking of a tunable extended-cavity diode laser to a cavity fringe without an expensive external modulator by simply modulating the laser.[21] The modulation width can be small compared with the cavity linewidth, and the modulation rate needs only to be large compared with the desired feedback bandwidth. However, the associated intensity modulation often causes a slight offset from line center that may change with time and, for instance, with the position and temperature of the cable wiring to the laser. Designing the system such that the required stability is roughly equivalent to the fringe width makes this issue unimportant, along with similar problems that are due to rf pickup. We used a DFB diode laser as our test laser and locked it to the *p*-polarized mode at 1479.4153 nm (mode line width,$\approx$3.8 MHz). The in-

jection current of the DFB diode laser was modulated at 28 MHz, and we checked the offsets that were due to intensity noise and rf pickup by moving the system cables and then measuring the absolute laser frequency. All offset related frequency changes were less than ± 100 kHz, equivalent to $\Delta\lambda/\lambda \leq 5 \times 10^{-10}$.

Optical alignment is another factor that can affect the test laser's frequency relative to the cavity-mode center. The spatial coupling to the cavity mode was excellent because of the use of single-mode fiber before the cavity, with more than 97% of the laser power coupled to the fundamental mode. As small alignment changes occur as a result of mechanical drift of the input mirrors, we expect slight changes of the residual transverse mode amplitudes. If one of the modulation sidebands is perturbed by such changes of a nearby transverse mode, the resultant imbalance will act to shift the laser slightly from line center. We checked the possible magnitude of such a misalignment-induced frequency offsets by purposely misaligning the input beam. While the input beam was locked to a fundamental mode, we caused a gross misalignment that reduced the mode amplitude in half while it increased the coupling to many transverse modes. The optical frequency shifted by 300 kHz, equivalent to $\Delta\lambda/\lambda \leq 1.5 \times 10^{-9}$. The actual alignment-induced errors during our frequency measurements were certainly much less, as the power output of the cavity was monitored during measurements to ensure that it was always at the nominal level.

We also checked for an optical power dependence of the mode frequency, which could be due, for instance, to absorption in the dielectric coatings. As the circulating power was adjusted in steps from 11 to 57mW, no trend was observed in the measured frequency to the resolution limit of our present method of frequency measurement, ± 10 kHz, equivalent to $\Delta\lambda/\lambda \leq 1.5 \times 10^{-11}$.

B. Frequency-Comb Issues

We turn now to the measurement of the test-laser frequency with the fiber-laser based frequency comb. Several milliwatts of light from the DFB test laser was split by a fiber coupler and transmitted 200 m via single-mode fiber to a fiber-based femtosecond laser.[22] The femtosecond laser had a repetition rate of approximately 50 MHz that was locked to a laboratory synthesizer referenced to one of the hydrogen masers of the National Institute of Standards and Technology time scale.[23] We give only a cursory explanation of the femtosecond comb laser measurements here, as the techniques have been well established.[24] The frequency comb output was mixed with the DFB power in a fiber coupler and filtered by a grating spectrometer (bandwidth, ~1 nm FWHM). The signal-to-noise ratio of the resultant beat note was limited by noise on the frequency comb, not by the available power from the DFB laser (which in fact was attenuated to prevent detector saturation). The feedback loop that was locking the DFB laser to the cavity mode had a bandwidth of approximately 200 kHz, limited by a slow response time internal to the laser package. Consequently there was little narrowing of the emission spectrum, and we observed beat notes approximately 1.9 MHz wide, as shown in Fig. 4. The contribution to the observed width from the comb mode is relatively small, as the synthesizer noise-limited jitter of the comb mode (mode index, $N \sim 4 \times 10^6$; see below) was less than 500 kHz. The DFB laser frequency is obtained from the rf beat note (f_{BEAT}) through

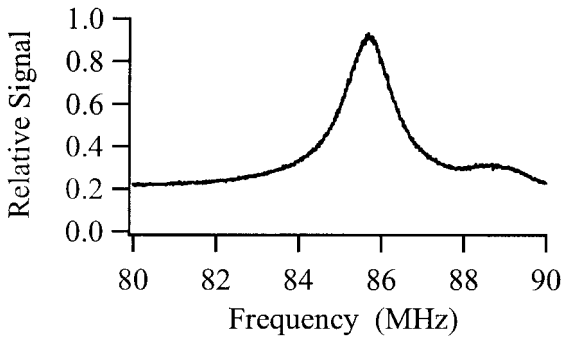

Fig. 4. Typical rf heterodyne beat note between the laser (locked to a cavity mode in vacuum) and a femtosecond laser comb mode. The spectrum analyzer averaged 300 readings (100 kHz resolution bandwidth) in approximately 6 s. We fitted the center portion of the beat note to a Lorentzian curve to extract the line center. The repeatability of this process was ± 10 kHz, equivalent to $\Delta\lambda/\lambda \leq 1.5 \times 10^{-11}$.

$$\nu_{\mathrm{DFB}} = N f_{\mathrm{REP}} \pm f_{\mathrm{CEO}} \pm f_{\mathrm{BEAT}}. \quad (2)$$

Here N is the femtosecond comb mode number, f_{REP} is the known femtosecond laser repetition rate, and f_{CEO} is the carrier-envelope offset frequency that is locked to a synthesizer. One can easily determine the signs of f_{BEAT} and f_{CEO} by slightly shifting the repetition rate and the offset frequency and observing the resultant frequency shift of the beat note. We are thus left with unambiguously determining mode index number N.

We determined index N by comparing the possible discrete DFB frequencies predicted by Eq. (2) with a seven-digit commercial wavelength meter reading of the DFB light. Such a procedure would be straightforward with a much larger femtosecond comb repetition rate but problematic here, as the absolute accuracy of the wavelength meter was specified at ± 40 MHz (2σ) at 1.48 μm. To solve this problem we calibrated the wavelength meter to the last digit (± 13 MHz) by measuring a nearby frequency that was well known. The reference was a 1.56 μm laser that was frequency doubled and locked to a rubidium transition at 780 nm.[25] We avoided alignment issues by calibrating and using the wavelength meter with a single-mode fiber patch cable permanently attached to the input.

4. Frequency and Wavelength Measurements

We tracked the (vacuum) frequency of one particular mode of the prototype wavelength reference for many months. During this time there was no temperature control, the cavity was often removed from the vacuum chamber, and on five occasions mirror cleanings were performed. Zerodur is well known to have thermally induced mechanical hysteresis,[26] and the temperature excursions could have been as much as ±5 °C. (The temperature was not monitored constantly but only during measurements.) The first measurement was made approximately nine months after the mirrors were optically contacted to the spacer. Sometimes measurements were performed on almost a daily basis; at other times there were weeks between measurements, notably during a time in November–December 2004 when the frequency comb was unavailable. For all frequency measurements the cavity was in a chamber with only moderate vacuum requirements (pressure, ≤0.1 Pa). The index of air at $\sim 10^5$ Pa is of the order of $n - 1 \approx 2 \times 10^{-4}$ so calculating the mode wavelength from a frequency measurement performed at 0.1 Pa results in a wavelength error of no more than $\Delta\lambda/\lambda \leq 2 \times 10^{-10}$.

We arbitrarily chose a TEM_{00} mode to measure and easily returned to the same mode at 1479.4153 nm for each measurement by using the wavelength meter, although the solid-state DFB laser was repeatable enough that the mode determination could also be accomplished by use of diode temperature and current. In terms of the diode parameters, the 1.19 GHz (0.0087 nm) free-spectral-range cavity modes were separated by 2 mA and 0.45 °C. In practice, when a less-repeatable tunable laser such as an extended-cavity diode laser is used, the proper mode can be determined with an auxiliary cavity, as mentioned above.

Preliminary optical frequency measurements were taken in an effort to map out the behavior of the mode center frequency with temperature. Heating tape and a cooling water jacket were installed on the outside of the vacuum chamber to change the cavity temperature, primarily by radiative means (the cavity was placed on a 1 mm thick Teflon sheet on an aluminum surface in the center of the chamber). In this manner we could adjust the cavity temperature in the range 18−28 °C. However, we found that mode frequency measurements while the cavity temperature was ramped were much less repeatable than when the temperature was held constant for an extended period of several hours. Unless the cavity is isothermal the average temperature reading of the six sensors does not uniquely correspond to the temperature distribution of the cavity structure, nor to the mode path length. In general, monitoring the effective temperature and subsequent expansion of a very low-thermal-conductivity structure by point temperature sensors is difficult because localized heating or cooling between sensors is not detected.

All the optical frequency measurements made after 30 June 2004 are shown in Fig. 5. To analyze the predictability of the wavelength reference we have normalized the data with respect to temperature and time. We assume that the two processes are independent, i.e., that the coefficient of thermal expansion is time invariant and the aging rate is (to first order) independent of temperature. In fact, the aging rate probably is temperature dependent; however, as the data are all within ±5 °C of room temperature, the assumption remains reasonable. The fit parameters (temperature and aging) were iterated to minimize the standard deviation of the entire corrected data set.

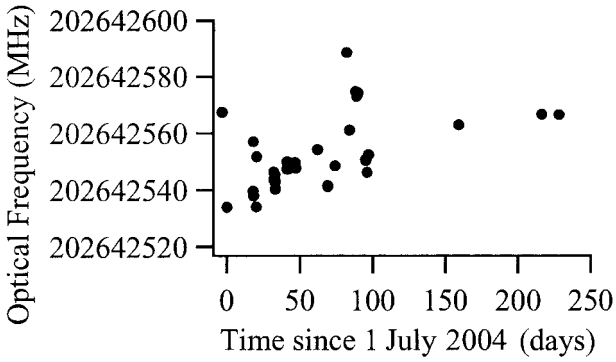

Fig. 5. This plot of all the frequency measurements performed versus time makes little intuitive sense, as there was no temperature control and, at least at first, there was rapid aging.

We normalize the data with respect to temperature by choosing a second-order expansion about an arbitrary temperature T_0:

$$\nu_{\mathrm{TempCorr}} = \nu_{\mathrm{Meas}}[1 + \alpha(T - T_0) + \beta(T - T_0)^2]. \quad (3)$$

We have found empirically that $\alpha = 42.2 \times 10^{-9}$ and $\beta = -0.5 \times 10^{-9}$ fit the data the best with $T_0 = 23$ °C. The cavity's linear coefficient of expansion (α) is slightly larger than the specified maximum for the bulk Zerodur material ($\alpha \leq \pm 30 \times 10^{-9}$). The measurements are shown in Fig. 6 normalized by Eq.

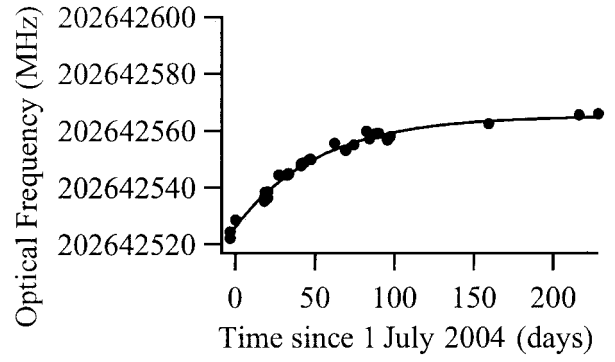

Fig. 6. Data from Fig. 5 corrected for the cavity's temperature by use of Eq. (3). The apparent logarithmic behavor is due to aging, and the data scatter is likely due to a poor approximation of the effective temperature of the optical path by the six point sensors, and also to thermal hysteresis of the Zerodur. The solid curve is an exponential fit to the data. The slope at day 240 has slowed down to 7.5 kHz/day, or $\Delta\nu/\nu = +1.35 \times 10^{-8}$/year.

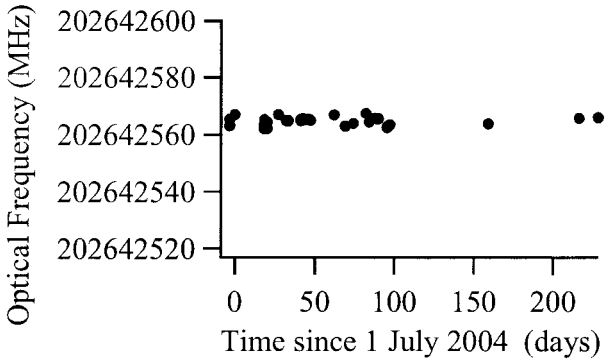

Fig. 7. Residuals after normalizing for temperature and aging. The data from Fig. 6 were normalized to day 240 by use of the best-fit exponential given in the text. The resultant frequency stability is ±4 MHz at 3σ, or $\Delta\nu/\nu \equiv 2 \times 10^{-8}$ (3σ).

(3) to $T_0 = 23$ °C. The solid curve is a least-squares fit to our assumed logarithmic aging process. The fit shows the optical frequency changing as $\nu_{\mathrm{Fit}} \approx \nu_0 - K_0 \exp(-\gamma \times \mathrm{days})$, with $K_0 = 39.1315$ MHz and $\gamma = 0.01916$ /day. Here, "days" refers to the number of days since midnight on 1 July 2004.

We next account for the aging process of the Zerodur cavity by normalizing the temperature-corrected frequency data to an arbitrary date, using these fitting parameters. We write

$$\nu_{\mathrm{Age\ \&\ TempCorr}} = \nu_{\mathrm{TempCorr}} - K_0[\exp(-\gamma t_0) - \exp(-\gamma \times \mathrm{days})] \quad (4)$$

to create the normalized data set $\nu_{\mathrm{Age\ \&\ TempCorr}}$ by increasing the frequencies measured before day t_0 and decreasing those measured after day t_0. The resultant data, normalized for temperature and aging, are given in Fig. 7. The scatter is ±4 MHz, or $\Delta\nu/\nu \cong 2 \times 10^{-8}$ (3σ). This represents our present statistical resolution, limited primarily, we believe, by our ability to measure the effective temperature of the cavity and by thermal hysteresis of the Zerodur. We suspect that a simpler structural design would result in better performance, allowing a handful of temperature sensors fixed to discrete points to approximate more closely the effective temperature of the cavity path length. That problem was compounded by the cavity's relatively high (42.2 parts in 10^9/°C) coefficient of thermal expansion.

In use, the wavelength of the reference cavity mode would be calculated in a manner similar to our use of Eqs. (3) and (4), decreasing the reported wavelength with time after calibration for aging and adjusting the reported wavelength proportionately for temperatures different from the temperature at calibration.

As mentioned above, the reported wavelength will also have a small dependence on atmospheric pressure, decreasing slightly as the cavity is compressed isotropically. Our ability to measure that change limits the accuracy of the wavelength reference. Two frequency measurements were recorded with the test laser locked to the same longitudinal mode of the cavity. During the first measurement (ν_1) the cavity was in vacuum (pressure, ≤0.1 Pa). A known pressure of (99.999% pure) helium gas measured with a capacitance manometer was then slowly introduced to the chamber, and a second measurement (ν_2) was performed after the temperature was allowed to stabilize for 30 min. The helium pressure was limited by the pressure gauge's dynamic range (13332 Pa or 100 Torr full scale), and the results were extrapolated to atmospheric pressure. We used the cavity temperature as the temperature of the helium gas in the cavity. We denote the refractive index at frequency ν_2 in the chamber as n and write

$$\lambda_2 = \frac{c}{n\nu_2}.$$

We recognize that the partial pressure of water owing to outgassing was certainly rising once the pump was closed off, because the chamber was never pumped beyond a moderate vacuum and never baked out. We account for outgassing by previously measuring the logarithmic rate of pressure change with time in the evacuated chamber (total pressure, 1.1 Pa after 30 min) and assuming that this pressure change was due to (and had the refractive index of) humid air. The resultant correction to the helium index is smaller than the uncertainty that is due to the gas temperature (see Table 1).

We can compare the mode wavelength under vacuum and isotropic pressure conditions by using Eq. (3) to normalize the frequency measurements in Table 1 to the same temperature. Although the temperature sensors bonded to the cavity have an absolute uncertainty of ±0.4 °C, the readout resolu-

Table 1. Summary of Data Used to Calculate the Atmospheric Pressure Compression of the Zerodur Cavity[a]

Measured Frequency (MHz)	Cavity Temperature (°C)	Helium Partial Pressure (Pa)	Outgassing Partial Pressure (Pa)	Refractivity ($n - 1$)
202642521.337	23.460	<0.1	<0.1	$<2.6 \times 10^{-10}$
202641686.058	23.590	13313(7)	1.1	$4.1937 \pm 0.0056 \times 10^{-6}$

[a]The refractivity given is the sum of the helium contribution and that which is due to outgassing in the chamber. The contribution to the refractivity from the helium partial pressure is $n - 1 = 4.1909\ (\pm 0.0056) \times 10^{-6}$, where the uncertainty is due to the gas absolute-temperature uncertainty (±0.4 °C) and the absolute-pressure uncertainty (±0.05%). The temperature uncertainty of the helium contribution is larger than the refractivity contribution from the outgassing, $n - 1 \cong 2.8 \times 10^{-9}$. Using the measured temperature coefficient (see text), we found that the +130 mK temperature difference between measurements accounts for −1.11 MHz of the frequency change.

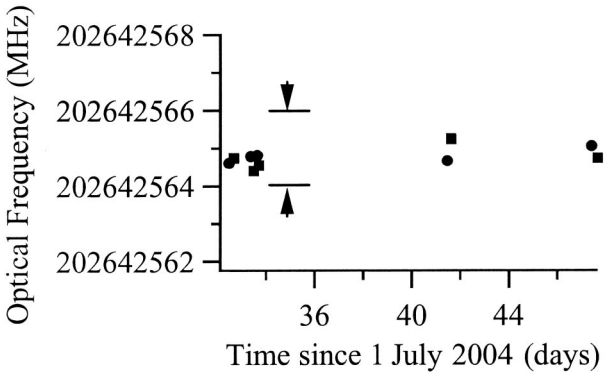

Fig. 8. Subset of ten measurements from Figs. 5–7 that were performed immediately before and after cleaning a cavity mirror (circles, before the cleaning; squares, after). All the measured frequencies have been normalized for temperature and time to 23°C and day 240, respectively. Arrows show a frequency difference equivalent to $\Delta\lambda/\lambda = 10^{-8}$. As the frequencies appear more-or-less randomly perturbed, it is possible that the changes in the measured frequencies are simply the residuals after temperature correction and are not related to the cleaning process.

tion is 1 m°C. At an indicated cavity temperature of 23.590 °C, the optical frequency and index-of-refraction data in Table 1 imply a mode wavelength of 1479.4153649 (7) nm in vacuum and 1479.415252 (8) nm at an isotropic pressure of 13,314 Pa. The uncertainties are due to uncertainties in frequency measurement (±100 kHz) and gas temperature (±0.4 °C), respectively. If we assume a linear contraction with pressure and extrapolate the wavelength (and uncertainty) to STP, the mode wavelength would become smaller than the vacuum value by 0.87(6) pm, or a proportional shift of $-5.9(4) \times 10^{-7}$, which is within 3% of the value calculated from theory by use of the normal Zerodur material parameters. An accurate pressure gauge with a 10^5 Pa full-scale range would have allowed us to avoid the assumption that cavity contraction is linear with pressure. The uncertainty of the wavelength at STP of ±0.06 pm or $\Delta\lambda/\lambda = \pm 4 \times 10^{-8}$, is due to uncertainty in the helium gas temperature.

At five different times we performed a mirror cleaning to see the effect on the measured frequency. For each test the mode frequency was recorded; then the cavity was removed from the chamber, and a mirror was cleaned by one or two swipes of optical tissue well moistened with anhydrous methanol. The cavity was then returned to the chamber, and the chamber was pumped to less than 0.1 Pa for a second measurement. The measurement pairs are all included in the previous data (Figs. 5–7), but we present them again in Fig. 8. We were not able to quantitatively measure a change of mode wavelength with mirror cleaning, as it appears that the measurement was limited by temperature-correction residuals.

In conclusion, we have demonstrated the calibration of an air wavelength reference by optical frequency measurements. The benefit of a physical cavity-based wavelength reference approach compared with the use of a frequency-stabilized laser and environmental air measurements appears to be higher accuracy and the possibility of supplying multiple known wavelengths to the interferometer user.

We thank W. C. Swann for periodic calibrations of the wavelength meter, J. Stone for useful discussions, and T. Heavner and T. Dennis for their careful reading of the manuscript. Specific product names are mentioned in this paper for technical clarity only and do not imply an endorsement.

References and Notes

1. P. D. Henshaw, P. Trepagnier, R. Dillon, W. Pril, and B. Hultermans, "Stage accuracy results using interferometers compensated for refractivity fluctuations," In *Optical Microlithography XVI,* A. Yen, ed., Proc. SPIE **5040,** 1672–1681 (2003).
2. C. R. Steinmetz, "Displacement measurement repeatability in tens of nanometers with laser interferometry," In *Integrated Circuit Metrology, Inspection, and Process Control II,* K. V. Monahan, ed., Proc. SPIE **921,** 406–420 (1988).
3. N. Bobroff, "Residual errors in laser interferometry from air turbulence and nonlinearity," Appl. Opt. **26,** 2676–2681 (1987).
4. P. E. Ciddor, "Refractive index of air: new equations for the visible and near infrared," Appl. Opt. **35,** 1566–1573 (1996).
5. M. L. Eickhoff and J. L. Hall, "Real-time precision refractometry: new approaches," Appl. Opt. **36,** 1223–1234 (1997).
6. R. Thibout, S. Topcu, Y. Alayli, and P. Juncar, "A transfer standard of the metre: an air wavelength reference," European Phys. J. Appl. Phys. **16,** 239–245 (2001).
7. S. Topcu, Y. Alayli, J.-P. Wallerand, and P. Juncar, "Heterodyne refractometers and air wavelength reference at 633 nm," European Phys. J. Appl. Phys. **24,** 8590 (2003).
8. J. A. Stone and A. Stejskal, "Wavelength-tracking capabilities of a Fabry–Perot cavity," in *Recent Developments in Traceable Measurements II,* J. Decker and N. Brown, eds., Proc. SPIE **5190,** 327–338 (2003).
9. R. Fox, K. Corwin, and L. Hollberg, "Stable optical cavities for wavelength references," NIST Tech. Note **1533** (2004).
10. S. A. Diddams, J. C. Bergquist, S. R. Jefferts, C. W. Oates, "Standards of time and frequency at the outset of the 21st century," Science **306,** 1318–1324 (2004).
11. M. Andersson, L. Eliasson, and L. R. Pendrill, "Compressible Fabry–Perot refractometer," Appl. Opt. **26,** 4835–4840 (1987).
12. P. H. Sneddon, S. Bull, G. Cagnoli, D. R. M. Crooks, E. J. Elliffe, J. E. Faller, M. M. Fejer, J. Hough, and S. Rowan, "The intrinsic mechanical loss factor of hydroxy-catalysis bonds for use in the mirror suspensions of gravitational wave detectors," Class. Quantum Grav. **20,** 5025–5037 (2003).
13. Product of Schott Glass. The mention of specific product names in this paper is for technical clarity and is not an endorsement.
14. Product of Corning Glass. The mention of specific product names in this paper is for technical clarity and is not an endorsement.
15. R. W. Boyd, "Intuitive explanation of the phase anomaly of focused light beams," J. Opt. Soc. Am **70,** 877–880 (1980).
16. J. A. Stone and A. Stejskal, "Using helium as a standard of refractive index: correcting errors in a gas refractometer," Metrologia **41,** 189–197 (2004).
17. F. Riehle, "Use of optical frequency standards for measurements of dimensional stability," Meas. Sci. Technol. **9,** 1042–1048 (1998).
18. L. Marmet, A. A. Madej, K. J. Siemsen, J. E. Bernard, and B. G. Whitford, "Precision frequency measurement of the $^2S_{1/2}$–$^2D_{5/2}$ transition of Sr^+ with a 674-nm diode laser locked

to an ultrastable cavity," IEEE Trans. Instrum. Meas. **46,** 169–173 (1997).
19. Chr. Tamm, D. Engelke, and V. Buhner, "Spectroscopy of the electric-quadrupole transition $^2S_{1/2}(F = 0)$–$^2D_{3/2}(F = 2)$ in trapped $^{171}Yb^+$," Phys. Rev. A **61,** 053405 (2000).
20. R. W. P. Drever, J. L. Hall, F. V. Kowalski, J. Hough, G. M. Ford, A. J. Munley, and H. Ward, "Laser phase and frequency stabilization using an optical resonator," Appl. Phys. B **31,** 97–105 (1983).
21. R. W. Fox, C. W. Oates, and L. Hollberg, "Stabilizing diode lasers to high finesse cavities," in *Cavity-Enhanced Spectroscopies,* Vol. 40 of Experimental Methods in the Physical Sciences, R. D. Van Zee and J. Looney, eds. (Syracuse U. Press, 2001).
22. B. R. Washburn, S. A. Diddams, N. R. Newbury, J. W. Nicholson, M. F. Yan, and C. G. Jorgensen, "Phase-locked, erbium-fiber-laser-based frequency comb in the near infrared," Opt. Lett. **29,** 250–252 (2004).
23. S. R. Jefferts, J. Shirley, T. E. Parker, T. P. Heavner, D. M. Meekhof, C. Nelson, F. Levi, G. Costanzo, A. De Marchi, R. Drullinger, L. Hollberg, W. D. Lee, and F. L. Walls, "Accuracy evaluation of NIST-F1," Metrologia **39,** 321–336 (2002).
24. J. L. Hall and J. Ye, "Optical frequency standards and measurement," IEEE Trans. Instrum. Meas. **52,** 227–231 (2003).
25. S. Gilbert, W. C. Swann, and T. Dennis, "Wavelength standards for optical communications," in *Laser Frequency Stabilization,* Standards, Measurements, and Applications, J. L. Hall and J. Ye, eds., Proc. SPIE **4269,** 184–191 (2001).
26. S. F. Jacobs, S. C. Johnston, J. M. Sasian, M. Watson, J. D. Targove, and D. Bass, "Surface figure changes due to thermal cycling hysteresis," Appl. Opt. **26,** 4438–4442 (1987).